

Level set based on new Signed Pressure Force Function for Echocardiographic image segmentation

Kalpana Saini¹, M.L. Dewal¹, and Manojkumar Rohit²

¹Deptt. of Electrical Engg., IIT Roorkee,
India

²Deptt. of Cardiology, PGIMER Chandigarh,
India

Copyright © 2013 ISSR Journals. This is an open access article distributed under the *Creative Commons Attribution License*, which permits unrestricted use, distribution, and reproduction in any medium, provided the original work is properly cited.

ABSTRACT: In the present paper a novel region based active contour method is developed by formulating a new signed pressure force (SPF) function. The method has been applied to the echocardiographic images for getting the desired boundary. The method is useful for finding the automatic boundary detection of other images (Microbiological, MRI, CT, Natural and welding joint etc.) as well. Level set method in combination with original SPF has not been able to give satisfactory results during the segmentation of echocardiographic images. There are lots of noises present in the echocardiographic images those create difficulties in the segmentation process. The proposed method resolves all these difficulties in such a manner that the output image is having the proper boundary detection without any disturbances and noises. The very important advantage of this method is that it gives a very fast response in terms of time taken by CPU and the number of iterations. Fast response is very important in the clinical area especially in diagnosis purpose. The presented model is an advancement of Selective Binary and Gaussian Filtering Regularized Level Set (SBGFRLS) method. Proposed model is more robust against images with weak edge and intensity inhomogeneity when compared with the performance of earlier methods.

KEYWORDS: Echocardiographic, Active contour, Signed pressure force function, Level set, Segmentation, Gaussian filtering, Regularized level Set.

1 INTRODUCTION

Segmentation is a well-known step which is carried out for the clinical diagnosis from medical images. But the major problem encountered during the segmentation of echocardiographic images. The literature shows that the active contour based segmentation techniques are being extensively used in medical imaging [1-5]. Active contour models can be categorized as edge based active contour models [1-4, 6, 9, 10, 11] and region based active contour models [5, 7, 8, 12-14].

Some of the edge based active contour models are used as the edge-detector. The operation of edge detector depends on the gradient of the image to stop the initial contour on the boundary of the interested objects. This technique has advantage when the objects and background of segmented image are heterogeneous. Drawbacks of these active contour models are that the satisfactory results cannot be achieved in case of objects with discrete or with the presence of blur boundaries or noise. Some active contour models as in [6] introduce the balloon force to shrink and enlarge the capture range of the force. However some undesired effects occur during balloon method. If weak balloon force is there then contour is not able to pass through the narrow part of the object, and if the balloon force is large, the contour will pass through the weak edges of the object. The geodesic active contour (GAC) [4] is the most popular methods in this category. This method uses an edge stopping function (ESF) which stops the contour on the object boundaries.

Region based active contour models have several advantages over edge based active contour models. Region based active contour models use the statistical information inside and outside the initial curve to evolve the contour towards the boundaries of the desired object. This renders it the less sensitive to noise and gives better performance in case of weak edges. It is also suitable for regions having no edges. Another advantage is the less sensitivity about the location of the initial contour to make it, in turn, easy to detect exterior and interior boundaries efficiently. The most popular method based on the Mumford- Shah model [14], in the category of region based active contour without edges is given by Chan-Vese (C-V)[5].

There are some hybrid models that are proposed in literature to drive the advantages of both GAC and C-V models. In [15] a geodesic-aided C-V (GACV) model had been proposed which includes region and local detector in the level set flow function. In [16] a variation method has been proposed using discriminating function for color image segmentation. In [17], the region was combined with the photometric invariant edge information for color-texture image segmentation. In [18] an integrated model is established by combining the edge location with statistical region information. Recently, in [19] signed pressure force function active contour model has been proposed. This model has the advantages of both GAC and C-V models.

In this paper, a level set method for active contour model is developed with a new signed pressure force function. Proposed model is faster than the model proposed in [19]. This model also gives the good segmentation which is represented in terms of graphical form in the paper. This model is used for Echocardiographic images in this paper but it is equally useful for other images also.

2 MATERIAL AND METHODS

2.1 GAC MODEL

In this model active contours evolve according to the measures that belong to intrinsic geometrics of the image [2, 4]. Splitting and merging takes place for the simultaneous detection both in exterior and interior boundaries. Geodesic active contour approach is based on the computation of geodesics or minimal distance curves. This allows the connection between classical snakes which are based on energy minimization and geometric active contours which are based on the theory of curve evolution. Level set formulation for GAC model is given by

$$\frac{\partial \phi}{\partial t} = g |\nabla \phi| \left(\operatorname{div} \left(\frac{\nabla \phi}{|\nabla \phi|} \right) + \alpha \right) + \nabla g \cdot \nabla \phi \quad (1)$$

Where ϕ is the level set function, ∇ is the gradient operator, α is real constant called the balloon force which controls the curve evolution and g is the edge based function and defined as in eq. (2)

$$g(|\nabla I|) = \frac{1}{1 + |\nabla G_\sigma * I|^2} \quad (2)$$

Where, σ is the standard deviation, $G_\sigma * I$ shows the convolution between image and the Gaussian kernel.

Because GAC model is based on gradient information so it is not suitable for images with weak edges. In some cases balloon force, which is very difficult to design has been used. The other weak balloon force doesn't allow the contour to pass through narrow part of the object and in case of the large balloon force, contour will pass through the weak edges. When contour is far from the object boundary then also it is difficult to find interior or exterior boundaries of the object.

2.2 C-V MODEL

Considering the problems of edge based models, Chan-Vese [5] proposed a region based active contour model which is a special case of Mumford-Shah formulation [14]. Level set equation for C-V model is as follows:

$$\frac{\partial \phi}{\partial t} = \delta(\phi) \left[\mu \nabla \left(\frac{\nabla \phi}{|\nabla \phi|} \right) - \lambda_1 (I(x, y) - c_1)^2 + \lambda_2 (I(x, y) - c_2)^2 \right] \quad (3)$$

Where $I(x, y)$ is the original image and $\mu \geq 0, \lambda_1 \geq 0, \lambda_2 \geq 0$ are constants. μ is related to smoothness and λ_1 and λ_2 are the external forces to drive the contour towards the object boundaries. $\delta(\phi)$ is the Dirac delta function. c_1 and c_2 are average intensities inside and outside of the object boundaries respectively and defined as:

$$c_1 = \frac{\int_{\Omega} I(x, y) \cdot H(\phi) dx dy}{\int_{\Omega} H(\phi) dx dy} \tag{4}$$

$$c_2 = \frac{\int_{\Omega} I(x, y) (1 - H(\phi)) dx dy}{\int_{\Omega} (1 - H(\phi)) dx dy} \tag{5}$$

Where $H(\cdot)$ is Heaviside function and Ω is a bounded open subset of R^2 .

C-V model is good boundary detection method but it takes more time to converge and gives unsatisfactory boundaries in case of echocardiographic images.

2.3 SBFRLS MODEL

Selective Binary and Gaussian filtering regularized level set (SBGFRLS) [19] utilizes the advantages of both GAC and C-V model. In the substitution of Edge Stopping Function (ESF), a region based Signed Pressure Force function has been (SPF) developed. This SPF function controls the direction of evolution. Opposite signs (range of SPF function is [-1 1]) around the boundaries of the object in this function make the contour to able to expand when it is inside the boundary and to shrinks when it is outside the boundary.

SPF function proposed in this model is as in eq. (6):

$$spf(I(x, y)) = \frac{I(x, y) - \frac{c_1 + c_2}{2}}{\max\left(\left|I(x, y) - \frac{c_1 + c_2}{2}\right|\right)}, x, y \in \Omega \tag{6}$$

Where c_1 and c_2 are defined in eq. (4) and (5) respectively.

On the substitution of SPF function in eq. (1), the level set formulation takes the form as in eq. (7)

$$\frac{\partial \phi}{\partial t} = spf(I(x, y)) \cdot \left(\operatorname{div} \left(\frac{\nabla \phi}{|\nabla \phi|} \right) + \alpha \right) |\nabla \phi| + \nabla spf(I(x, y)) \cdot \nabla \phi, x, y \in \Omega \tag{7}$$

The regular term $\operatorname{div} \left(\frac{\nabla \phi}{|\nabla \phi|} \right) |\phi|$ is un-necessary because Gaussian filter can be utilized to smooth the level set function to keep the interface regular. Also the term $\nabla spf \cdot \nabla \phi$ can be removed because the method utilizes the statistical information of the regions. Thus the final level set model is given as in eq. (8)

$$\frac{\partial \phi}{\partial t} = spf(I(x, y)) \cdot \alpha |\nabla \phi|, x, y \in \Omega \tag{8}$$

2.4 THE PROPOSED MODEL

The SBFRLS model is able to overcome the problems of the GAC and the C-V model but still it is not good for echocardiographic images. It is not able to detect all boundaries. So here in the proposed model a new SPF function

$spf_n(I(x, y))$ is developed to overcome this problem. Proposed model also takes less time to converge and the lesser number of iterations to converge when compared with other models.

$$spf_n(I(x, y)) = \frac{\left((c_1 * c_2) * \left(I(x, y) - \frac{c_1 + c_2}{2} \right) \right)}{\max \left(\left((c_1 * c_2) * \left(I(x, y) - \frac{c_1 + c_2}{2} \right) \right) \right)}, x, y \in \Omega \tag{9}$$

Where $spf_n(I(x, y))$ is the new SPF function as explained in the proposed method.

The significance of new SPF explained in eq. (9) can be explained by referring fig. (1), which explains that $Min(I(x, y)) \leq c_1, c_2 \leq Max(I(x, y))$. Hence

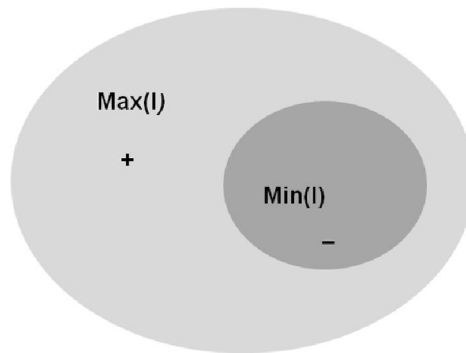


Fig. 1. Signs of SPF function inside and outside of the object

$$Min(I(x, y)) < (c_1 * c_2) \frac{c_1 + c_2}{2} < \max(I(x, y)), x, y \in \Omega \tag{10}$$

Due to identical signs of the new SPF function in eq. (9) and in fig.1 eq. (9) can be used as SPF function. So substituting the new SPF function in the eq. (1), we get the level set formulation as expressed in eq. (11)

$$\frac{\partial \phi}{\partial t} = spf_n(I(x, y)) \cdot \left(\operatorname{div} \left(\frac{\nabla \phi}{|\nabla \phi|} \right) + \alpha \right) |\nabla \phi| + \nabla spf_n(I(x, y)) \cdot \nabla \phi, x, y \in \Omega \tag{11}$$

Similar to SBFRLS model, the regular term $\operatorname{div} \left(\frac{\nabla \phi}{|\nabla \phi|} \right) |\phi|$ and $\nabla spf_n \cdot \nabla \phi$ can be removed because of the similar reasons as explained earlier. The final level set equation for the proposed method thus given in eq. (12)

$$\frac{\partial \phi}{\partial t} = spf_n(I(x, y)) \cdot \alpha |\nabla \phi|, x, y \in \Omega \tag{12}$$

2.5 STATISTICAL PARAMETERS USED FOR PERFORMANCE ANALYSIS

For getting the performance of the method statistical analysis has been done on the population of time taken per iterations. The four parameters mean, median, standard deviation and variance have been calculated.

Mean is defined as

$$\mu = \sum t / n \tag{13}$$

Where μ is the symbol for representing mean and $\sum t$ is the sum of time ken for all the iterations and n is the number of total iterations taken for the boundary detection of particular image.

Median is related to the middle value of time from time population.

The variance is the average squared deviation from the group of time mean, as defined by the following formula:

$$\sigma^2 = \sum(t_i - \mu)^2 / n \tag{14}$$

Where σ^2 is the variance, μ is the mean and t_i is the i th element from the time population.

The standard deviation is the square root of the variance. Thus, the standard deviation is defined as:

$$\sigma = \sqrt{\sigma^2} = \sqrt{\sum(t_i - \mu)^2 / n} \tag{15}$$

3 RESULTS

All the echocardiographic images used in the present paper for the experiment purpose are taken from Post Graduate Institute of Medical Education and Research (PGIMER) Chandigarh, India. These images are from patients who were suffering from mitral regurgitation. Parasternal long axis and apical two and four chamber view are included for diagnosing the regurgitation by analyzing the size of chambers.

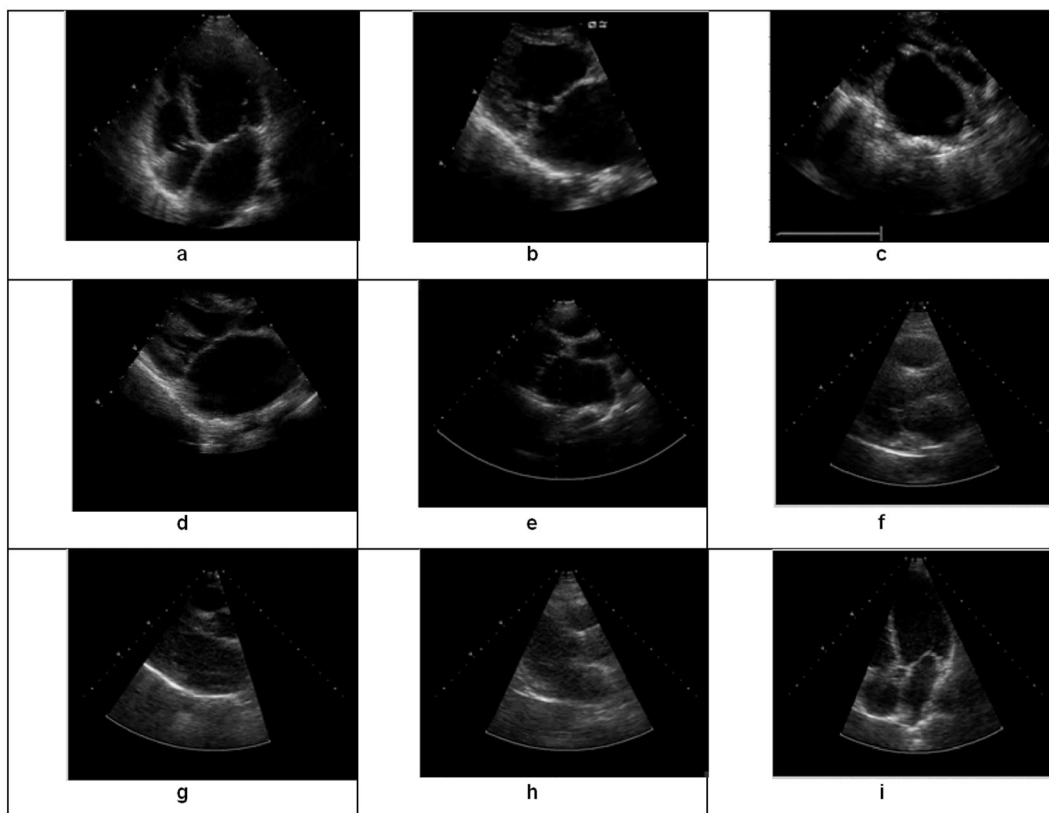


Fig. 2. Original echocardiographic Images showing the parasternal and apical view of the heart

Fig. 2. is the collection of original images associated with nine patients suffering from mitral regurgitation. Apical four views are in fig 2a and 2i. other images i.e. fig 2b, 2c, 2d, 2e, 2f, 2g and 2h are on parasternal long axis view.

Fig.3 shows the images after boundary detection with GAC model. In this figure it can be seen that from among the nine cases none gives the satisfactory boundaries. Contour leaks the required boundaries also.

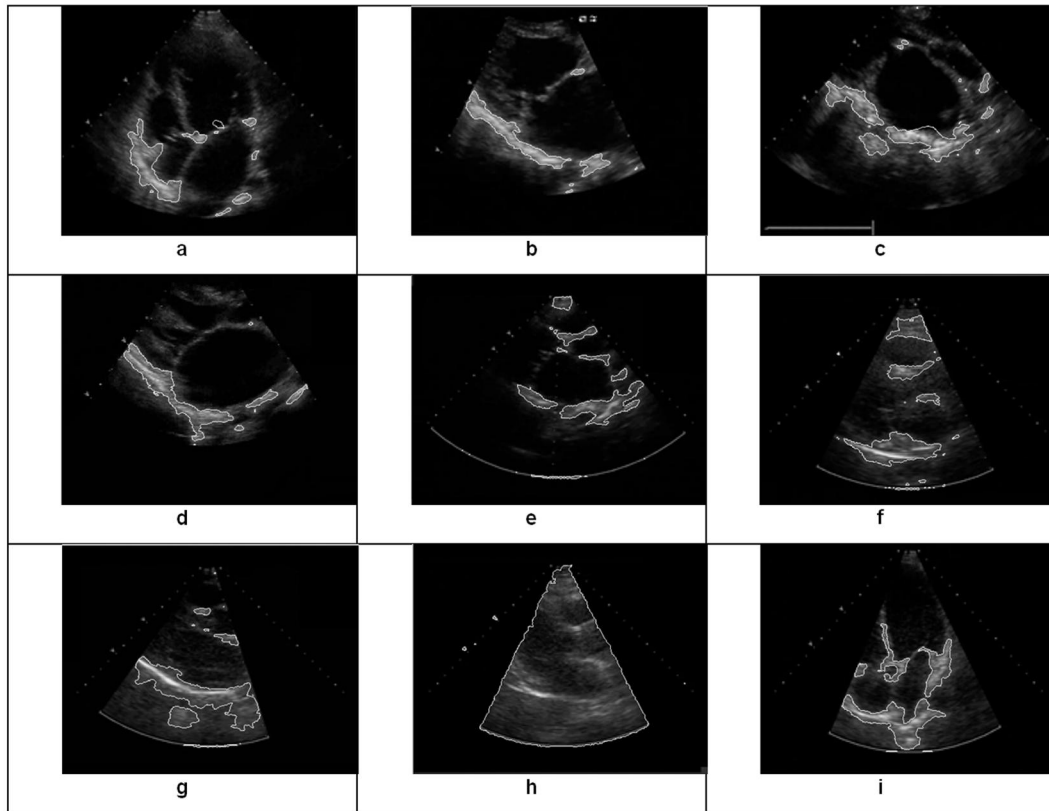


Fig. 3. *Boundary detection of echocardiographic images with GAC model*

Fig.4 shows the boundary detected images with C-V model. Here the results are better than the results obtained from the GAC model, However, here also the C-V model is not able to detect properly the boundaries of all the images. For example in fig 4a and fig 4i it is clearly seen that the contour is not able to detect all necessary boundaries and the similar deficiencies are also seen more or less in other images viz. fig. 4b to fig. 4h. So it is difficult to distinguish chambers properly.

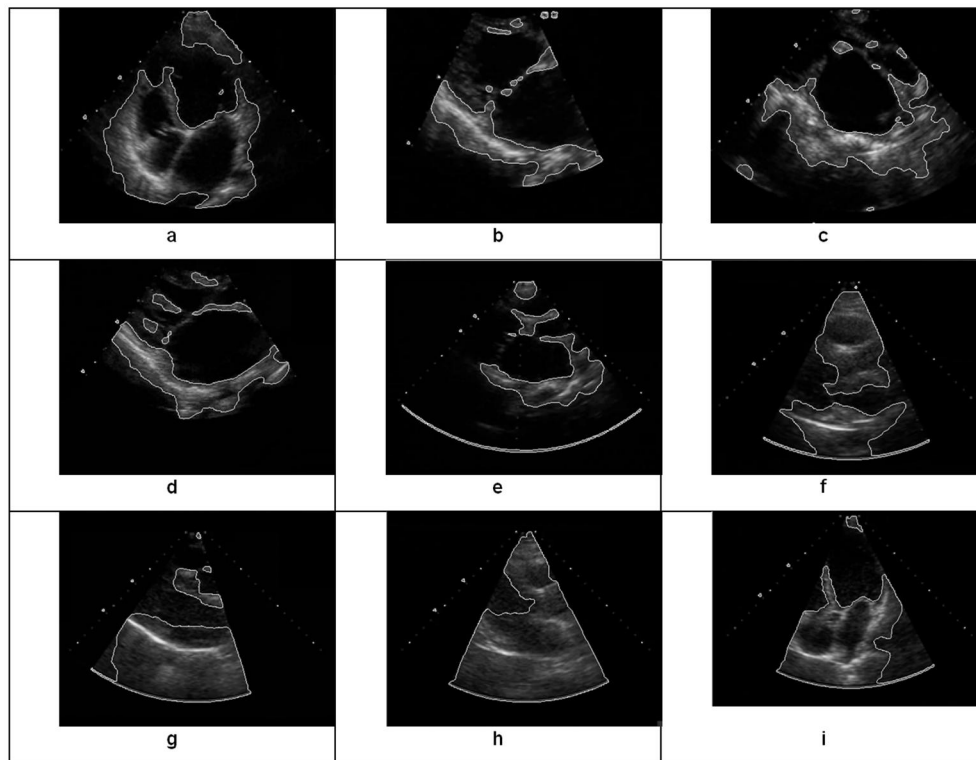


Fig. 4. Boundary detection of echocardiographic images with C-V model

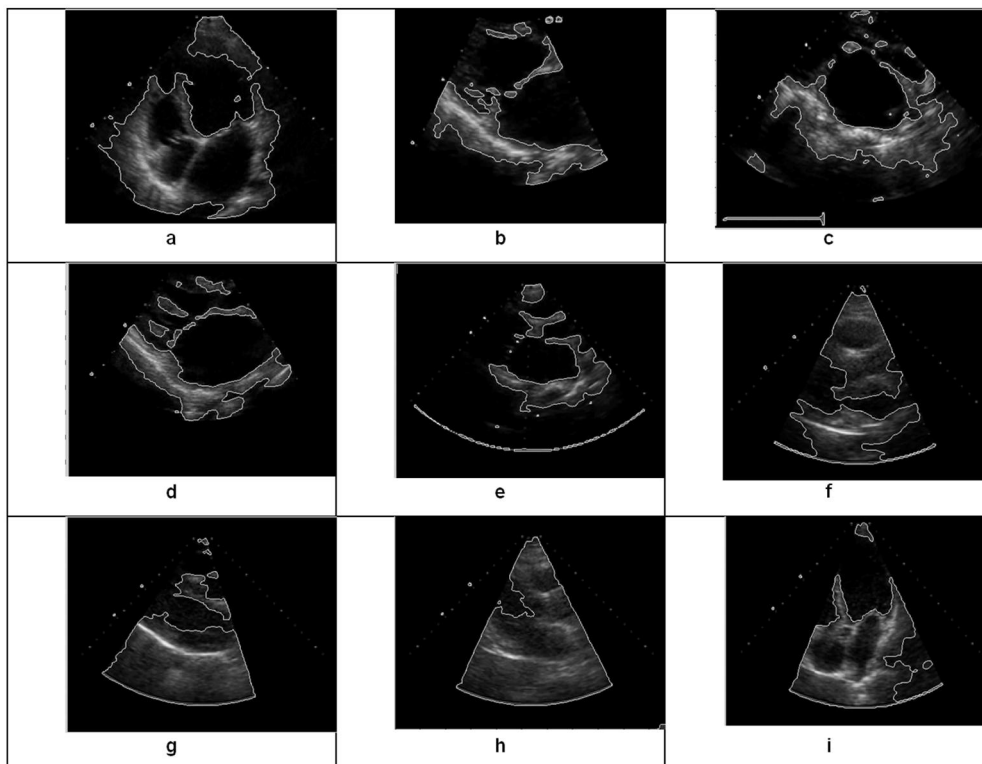


Fig. 5. Boundary detection of echocardiographic images with SBFRLS model

Fig. 6 is the results obtained using the proposed method. It can be seen that the proposed model is able to detect all chambers boundaries. A human eye can very efficiently detect the chambers of the heart from fig. 6a through 6i. The

proposed method has been able to detect the proper boundaries in those images also in which when processed through C-V and SBGFRLS models could not be detected. Such images are for example of (i) fig. 5a and 6a, (ii) fig. 5f and 6f, (iii) fig. 5h and 6h and for (iv) fig. 5i and 6i.

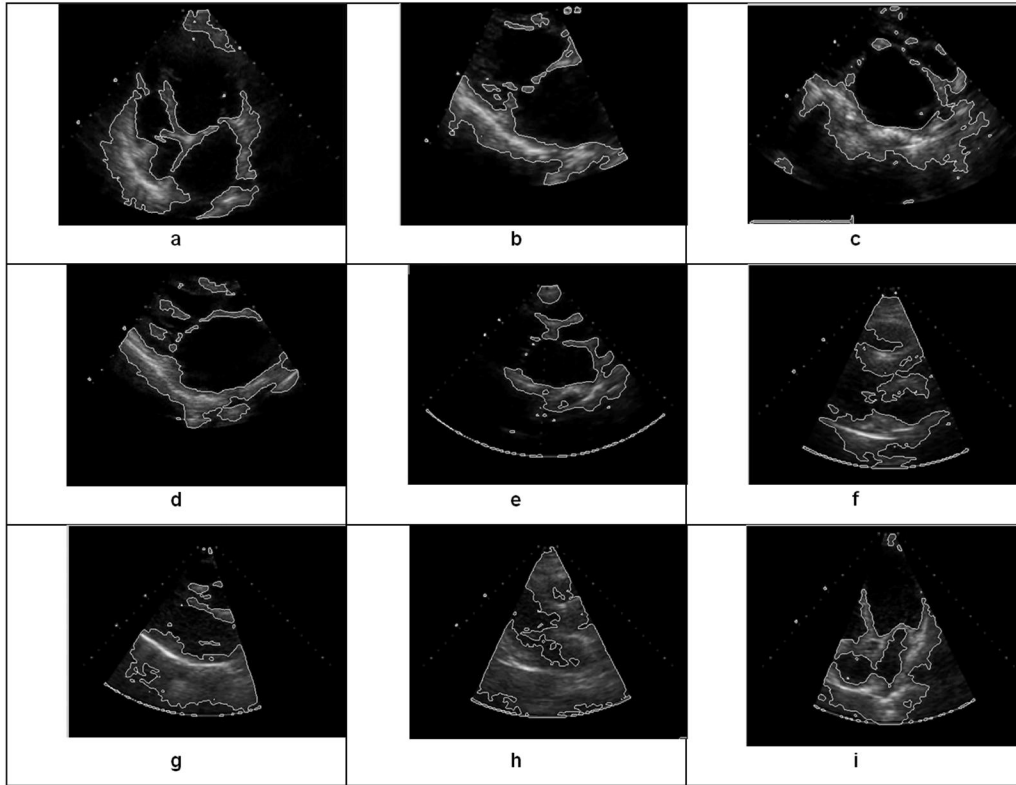


Fig. 6. Boundary detection of echocardiographic images with proposed model

4 DISCUSSION

The proposed model is also the most efficient when compared with the other models in terms of the number of iterations and time it takes to converge. It takes lowest time and iterations. Table 1 shows the iterations and time taken by GAC, C-V, SBGFRLS and the proposed model. From observations from the table 1 it is seen, whereas the GAC model, C-V model and The SBGFRLS models takes 1400 to 4000, 1500 to 2500 and 100 to 200 iterations respectively, the proposed model takes only 30 to 60 iterations to converge; and whereas these three models take the total time to converge ranging from 142.79 to 485.28 seconds, 34.01 to 62.80 seconds and 2.15 to 4.68 seconds respectively, the proposed model takes total time ranging from 0.64 to 1.13 seconds only.

Table 1. Comparison between GAC, C-V, SBGFRLS and proposed model based on CPU efficiency

Images	GAC Model		C-V Model		SBGFRLS Model		Proposed Model	
	Iterations	Time (sec.)	Iterations	Time (sec.)	Iterations	Time (sec.)	Iterations	Time (sec.)
1	2300	278.94	1500	36.35	150	3.32	40	0.81
2	2500	250.49	1800	44.19	150	3.24	40	0.75
3	2300	300.67	2500	62.86	100	2.15	30	0.64
4	2500	270.73	1900	40.75	150	2.86	40	0.73
5	2500	389.96	2000	47.98	200	4.68	50	0.95
6	3000	386.51	1800	43.61	150	2.96	50	0.96
7	4000	485.28	2000	46.47	200	4.16	40	0.76
8	1400	142.79	1500	34.01	150	2.89	60	1.13
9	3200	365.06	1600	36.84	200	4.29	50	0.95

The statistical analysis have also been done to show graphically as in figs. 7a, 7b, 7c and 7d for mean, median, standard deviation and variance respectively, for the per iteration time taken in GAC, C-V, SBGFRLS and the proposed model.

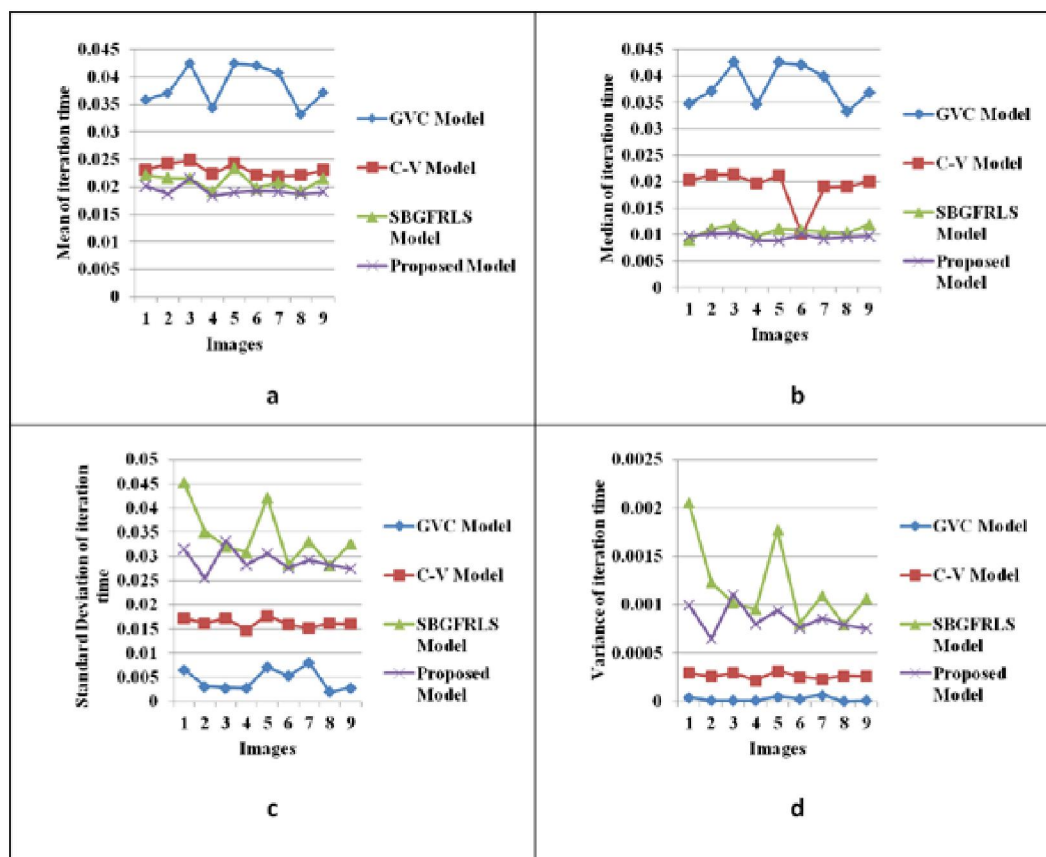


Fig. 7. Statistical analysis of the proposed model along with other models for the per iteration time taken to converge

5 CONCLUSION

The proposed model presents a method to detect boundaries of echocardiographic images automatically. Automatic detection of boundaries enables the clinicians to determine the chambers efficiently and carry out easy diagnosis. The proposed method is efficient in terms of detecting the proper boundaries with the highest clarity. It exhibits much higher CPU efficiency which is of very high significant to the clinicians for carrying out speedy diagnosis. The new SPF developed in this paper can also be used with all types of active contours.

REFERENCES

- [1] M. Kass, A. Witkin, D. Terzopoulos, "Snakes: active contour models," *International Journal of Computer Vision*, vol. 1, pp. 321–331, 1988.
- [2] V. Caselles, R. Kimmel, G. Sapiro, "Geodesic active contours," in: *Proceeding of IEEE International Conference on Computer Vision'95*, Boston MA, pp 694–699, 1995.
- [3] S. Kichenassamy, A. Kumar, P. Olver, A. Tannenbaum, "Conformal curvature flows: From phase transitions to active vision," *Arch. Ration. Mech. Anal.*, vol 134, no. 3, pp. 275-301, 1996.
- [4] V. Caselles, R. Kimmel, G. Sapiro, "Geodesic active contours," *International Journal of Computer Vision*, vol. 22, no.1, pp. 61–79, 1997.
- [5] Chan T, Vese L, "Active contours without edges," *IEEE Transaction on Image Processing*, vol. 10, no. 2, pp. 266–277, 2001.
- [6] G. P. Zhu, S. Q. Zhang, Q. S. Zeng, C. H. Wang, "Boundary-based image segmentation using binary level set method," *Optical Engineering* vol. 46:050501, 2007.

- [7] G. Zhu, S. Zhang, Q. Zeng, and C. Wang C, "Boundary-based image segmentation using binary level set method," *SPIE Letters*, vol.46, no. 5, 2007.
- [8] R. Ronfard, "Region-based strategies for active contour models", *Int. 1.Comp. Vis.*, vol.13, no. 2, pp. 229-251, 1994.
- [9] C. Samson, L. Blanc-Feraud, G. Aubert and J. Zerubia, "A variational model for image classification and restoration," *IEEE Trans. Patt. Anal. Mach. Intell.*, vol. 22, no. 5, pp. 460- 472, 2000.
- [10] C. M. Li, C. Y. Xu, C. F. Gui, M. D. Fox, "Level set evolution without re-initialization: a new variational formulation," in: *IEEE Conference on Computer Vision and Pattern Recognition*, San Diego, pp. 430–436, 2005.
- [11] N.Paragios, R. Deriche, "Geodesic active contours and level sets for detection and tracking of moving objects," *IEEE Transaction on Pattern Analysis and Machine Intelligence*, pp. 221–15, 2000.
- [12] C. Xu, J. L. Prince, "Snakes, shapes, and gradient vector flow," *IEEE Transaction on Image Processing*, vol. 7, pp. 359-369, 1998.
- [13] J. Lie, M. Lysaker, X. C. Tai, "A binary level set model and some application to Mumford–Shah image segmentation," *IEEE Transaction on Image Processing*, vol. 15:1171-1181.
- [14] Mumford D, Shah J, "Optimal approximation by piecewise smooth function and associated variational problems," *Communication on Pure and Applied Mathematics* 42, pp. 577-685, 1989.
- [15] L. Chen, Y. Zhou, Y. G. Wang and Yang, "GACV: geodesic-aided C-V method," *Pattern Recognition*, vol. 39, pp. 1391-1395, 2006.
- [16] L. Pi L, J. Fan and C.M. Shen, "Color image segmentation for objects of interest with modified geodesic active contour method", *Math. Image and Vis*, vol. 27, pp. 51-57, 2007.
- [17] S. Y. Yu, Y. Zhang, Y. Wang, and J. Yang, "Color-texture image segmentation by combing region and photometric invariant edge information," in: *MCAM 2007*, 4577, pp. 286-294, 2007.
- [18] Z. Ying, L. Guangyao, S. Xiehua, and X. Xinmin, "Geometric active contours without re-initialization for image segmentation," *Pattern Recogn.*, vol.42, no. 9, pp. 1970-1976, 2009.
- [19] K. Zhang, L. Zhang, H. Song, W. Zhou, "Active contours with selective local or global segmentation: A new formulation and level set method," *Image and Vision Computing* vol. 28, pp. 668-676, 2010.